IN THE NAME OF ALLAH

Shiraz University
Faculty of Engineering

Ph.D. Dissertation
In Chemical Engineering

THEORETICAL AND EXPERIMENTAL KINETICS STUDY OF GAS HYDRATE FORMATION IN THE PIPELINE

By
MOHAMMAD SARSHAR

Supervised by
PROF. J. FATHIKALAJAHI
DR. F. ESMAEILZADEH

June 2008

دانشکده مهندسی

پایان نامه دکتری در رشته مهندسی شیمی

بررسی تئوری و آزمایشگاهی تشکیل برفک گازی در خطوط لوله

توسط:

محمد سرشار

استاد راهنما:

دکتر جمشید فتحی کلجاهی

دکتر فریدون اسماعیل زاده

تیر ماه ۱۳۸۷

To Mahsa

and

Lovely Matin and Yasamin

IN THE NAME OF GOD

THEORETICAL AND EXPERIMENTAL KINETICS STUDY OF GAS HYDRATE FORMATION IN THE PIPELINE

BY:

MOHAMMAD SARSHAR

THESIS

SUBMITTED TO THE SCHOOL OF GRADUATE STUDIES IN PARTIAL FULFILLMENT OF THE REQUIREMENTS FOR THE DEGREE OF DOCTOR OF PHILOSOPHY (Ph.D.)

IN

CHEMICAL ENGINEERING

SHIRAZ UNIVERSITY
SHIRAZ
ISLAMIC REPUBLIC OF IRAN

EVALUATED AND APPROVED BY THE THESIS COMMITTEE, AS: EXCELLENT

J. FATHIKALAJAHI, Ph.D., PROF. OF CHEMICAL ENGINEERING (CHAIRMAN)

F. ESMAEILZADEH, Ph.D., ASSISTANT PROF. OF CHEMICAL ENGINEERING (CHAIRMAN)

D. MOWLA, Ph.D., PROF. OF CHEMICAL ENGINEERING

A. M. ALAMDARI, Ph.D., ASSOCIATE PROF. OF CHEMICAL ENGINEERING

M. KAZEMEINI, Ph.D., PROF. OF CHEMICAL ENGINEERING

JUNE 2008

Acknowledgments

Author appreciates financial supports of the thesis by National Iranian Oil Company and cooperation of Fars Engineering Research Center. Author greatly acknowledges Prof. J. Fathikalajahi and Dr. F. Esmaeilzadeh for their valuable scientific and technical supports as the supervisors of the thesis. Further, valuable advises of Prof. D. Mowla and Dr. A. M. Alamdari are also appreciated. Finally, the official supports of Dr. M. Hatam and Mr. R. Eqra, the managers of Fars ERC are appreciated.

ABSTRACT

THEORETICAL AND EXPERIMENTAL KINETICS STUDY OF GAS HYDRATE FORMATION IN THE PIPELINE

BY

MOHAMMAD SARSHAR

A flow loop setup has been developed for the kinetics study of gas hydrate formation in the gas pipeline. Experiments have been carried out for carbon dioxide, propane and a mixture of methane and propane at operating temperatures and pressures of 3-8 °C and 1-5 MPa. The above mentioned gases are selected because; they are the constituents of the natural gas. Hydrate formation rate is directly proportional to the gas consumption rate and due to this, the hydrate formation rate is determined by the measurement of the gas consumption rate. The measured gas consumption rates are in the range of 0.05-0.20 gr/s. Further, a set of partial differential and algebraic equations have been developed based on the crystallization, mass transfer, nucleation and equilibrium concepts to simulate the process of hydrate formation in the flow loop. The predicted gas consumptions are compared with the experimental data for which good agreements are achieved.

Table of contents

Title	Page
Chapter 1- Introduction	**1**
1-1- Hydrate structures	2
1-2- Hydrate equilibrium conditions	4
1-3- Mechanisms of gas hydrate formation	5
1-4- Driving forces of gas hydrate formation	7
1-5- Rate of gas hydrate formation	10
1-6- Size of the hydrate crystals	12
1-7- Nucleation and induction time models	14
1-8- Gas hydrate formation rate expression	15
1-9- Setup for the gas hydrate experiments	21
Chapter 2- Mathematical modeling of gas hydrate formation in the pipe	24
2-1- Mechanism of gas hydrate formation	24
2-2- Mathematical modeling of gas hydrate formation in a flow loop	25
2-3- The reaction rate expression	26
2-4- Nucleation rate expression	27

Title	Page
2-5- Growth rate expression	28
2-6- Driving force of the gas hydrate formation	29
2-7- Equilibrium hydrate calculations	30
2-8- Determining the gas consumption rate	32
2-9- Diffusivity	33
2-10- Fugacity	33
2-11- Henry's constants	34
2-12- Water specific volume	35
Chapter 3- Experimental setup	**36**
3-1- Discussion	36
3-2- Flow loop elements	38
3-2-1- Pipe	38
3-2-2- Mixing vessel	38
3-2-3- Screw Pump	39
3-2-4- Boosting pump	40
3-2-5- Cooling jacket	40
3-2-6- Magnetic flow meter	40
3-2-7- Gas storage tank	41
3-2-8- Mass flow meter	41
3-2-9- Pressure drop transmitter	43
3-2-10- Chilled water circuit	43
3-2-11- Temperature and pressure monitoring	44
3-3- Flow loop operation	45

Title	Page
Chapter 4- Simulation	47
4-1- Equilibrium calculations	47
4-1-1- Solution of the equation of states	47
4-1-2- Bubble point calculations	48
4-1-3- Dew point calculations	49
4-1-4- Pressure adjustment	49
4-1-5- Flash calculations	51
4-2- Hydrate equilibrium calculations	51
4-3- Kinetics calculations	53
4-3-1- Calculating supersaturation	53
4-3-2- Nucleation and growth rates	54
4-4- Flow loop calculations	55
Chapter 5- Results and Discussion	57
5-1- Equilibrium hydrate formation	57
5-2- Experimental data	60
5-2-1- CO2 hydrate formation	60
5-2-2- Propane hydrate formation	62
5-2-3- Hydrate formation of mixture of 73% methane and 27% propane	65
5-3- Simulation of hydrate formation	68
5-3-1- Simulation of CO2 hydrate formation	68
5-3-2- Simulation of propane hydrate formation	72
5-3-3- Simulation of 73% methane + 27% propane hydrate formation	77
5-4- Conclusion	82
References	83
Publications	89

List of Tables

Title	Page
Table 2-1- The Kihara parameters of equation (2-23)-(2-25) for some hydrate formers	32
Table 2-2- The macroscopic parameters of equation (2-26) for hydrates formation	32
Table 2-3- The parameters of equation (2-42) for some hydrate formers	35
Table 2-4- Parameters for of Jager equation	35
Table 3-1- Operating conditions of hydrate formation	46
Table 5-1- Gas composition of three natural gas mixtures	57
Table 5-2- Flow loop specifications	68

List of figures

Title	Page
Figure 1-1- Hydrate structures known as (a) structure I (SI), (b) structure II (SII) and (c) structure H (SH)	2
Figure 1-2- (a) Pentagonal Dodecahedron (5^{12}) (b) Tetrakaidecahedron ($5^{12}6^2$) (c) Hexakaidecahedron ($5^{12}6^4$)	3
Figure 1-3- A generalized solubility- supersolubility diagram. Continues line is the solubility and the broken line is the supersolubility curve	8
Figure 1-4 - Schematic representation of a reactor setup for hydrate formation	21
Figure 1-5- Schematic representation of a laboratory flow loop	22
Figure 1-6- Schematic representation of a pilot flow loop	23
Figure 1-7- Pilot flow loop of petroleum institute of France	23
Figure 2-1- Schematic representation element (i) at time (t)	25
Figure 2-2- Schematic representation of nucleus formation on a) solid substrate and b) at the liquid gas interface	28
Figure 2-3- Schematic representation of gas hydrate formation from aqueous phase	30

Title	Page
Figure 3-1- Laboratory flow loop for hydrate formation	37
Figure 3-2- Laboratory flow loop for hydrate formation	37
Figure 3-3- Stainless steel pipe used in the fabrication of the flow loop	38
Figure 3-4- Mixing vessel quipped with the cooling jacket	39
Figure 3-5- KRACHT screw pump	39
Figure 3-6- Piston pump used for the water injection	40
Figure 3-7- Endress Hauser magnetic flow meter	41
Figure 3-8- Pressure regulator	41
Figure 3-9-The pressure drop transmitter and the orifice plate	42
Figure 3-10- Orifice plate for the gas flow measurement	42
Figure 3-11-Rosemount pressure drop transmitter	43
Figure 3-12- Mixing chamber for producing the chilled water	44
Figure 3-13- Centrifugal pump for circulating the chilled water	44
Figure 3-14- Temperature monitoring system	45
Figure 3-15- Pressure gauge situated after the screw pump	45
Figure 4-1- Block diagram for equation of state solution	48
Figure 4-2- Block diagram for bubble point calculations	49
Figure 4-3- Block diagram for dew point calculations	50
Figure 4-4- Block diagram for pressure adjustment	50
Figure 4-5- Block diagram for flash calculations	51
Figure 4-6- Block diagram for hydrate equilibrium calculations	52
Figure 4-7- Block diagram for driving force calculations	53
Figure 4-8- Block diagram for nucleation and growth rates calculations	54
Figure 4-9- Block diagram for the solution of equations 4-1 to 4-5	56
Figure 5-1- Comparison of hydrate formation pressures calculated in this work and the results of CSMhyd and Hysys softwares	58

Title	Page
Figure 5-2- Comparison of hydrate formation pressures calculated in this work and the results of CSMhyd for gas mixture B	59
Figure 5-3- Comparison of hydrate formation pressures calculated in this work and the results of CSMhyd for gas mixture C	59
Figure 5-4- Flow loop temperature in the CO_2 experiment	61
Figure 5-5- Flow loop pressure in the CO_2 experiment	61
Figure 5-6- CO_2 consumption rate in the flow loop	62
Figure 5-7- Flow loop temperature in the propane experiment	63
Figure 5-8- Flow loop pressure in the propane experiment	63
Figure 5-9- Propane consumption rate in the flow loop	64
Figure 5-10- Flow loop pressure drop in propane experiment	64
Figure 5-11- Flow loop temperature in the experiment with the mixture of methane and propane	66
Figure 5-12- Flow loop pressure in the experiment with the mixture of methane and propane	66
Figure 5-13- 73% methane + 27% propane consumption rate in the flow loop	67
Figure 5-14- Flow loop pressure drop in the experiment with the mixture of methane and propane	67
Figure 5-15- Nucleus size as a function of pressure and wetting angle at 279.65 (K)	68
Figure 5-16- Work for nucleus formation as a function of pressure and wetting angle at 279.65 (K)	69
Figure 5-17- Nucleation rate as a function of pressure and wetting angle at 279.65 (K)	70
Figure 5-18- Driving force of hydrate reaction as a function of pressure	71

Title	Page
Figure 5-19- ψ factor as a function of wetting angle	71
Figure 5-20- Measured and calculated CO_2 consumptions at 4.9 MPa and 279.65 (K) in a hydrate flow loop	72
Figure 5-21- Nucleus size as a function of pressure and wetting angle at 276.65 (K)	73
Figure 5-22- Work for nucleus formation as a function of pressure and wetting angle at 276.65 (K)	73
Figure 5-23- Nucleation rate as a function of pressure and wetting angle at 276.65 (K)	74
Figure 5-24- Driving force of hydrate reaction as a function of pressure at 276.65 (K)	75
Figure 5-25- ψ factor as a function of wetting angle	75
Figure 5-26- Measured and calculated propane consumptions at 4.9 MPa and 279.65 (K) in a hydrate flow loop	76
Figure 5-27- Nucleus size as a function of pressure and wetting angle at 277.65 (K)	77
Figure 5-28- Work for nucleus formation as a function of pressure and wetting angle at 277.65 (K)	78
Figure 5-29- Nucleation rate as a function of pressure and wetting angle at 277.65 (K)	79
Figure 5-30- Driving force of hydrate reaction as a function of pressure at 277.65 (K)	80
Figure 5-31- ψ factor as a function of wetting angle	80
Figure 5-32- Measured and calculated CH_4+C_3H_8 consumptions at 2.0 MPa and 277.65 (K) in a hydrate flow loop	81

Nomenclature

a	Surface area (m^2)
A	Kinetics parameter
b	Shape factor
c	Parameter of equation (2-10)
C	Concentration (mol/m^3)
D	Diffusivity (m^2/s)
d	Pipe diameter (m)
f	Fugacity (bar)
G	Growth rate
J	Nucleation rate (m^{-3} s or m^{-2} s)
k	Boltzman constant
Mw	Molecular weight
Na	Avogadro number
n	Mole number (mole)
ṅ	Hydrate building units
n_w	Hydration number
P	Pressure (bar)
q	Consumption (mole)
rc	Crystal radius (m)
R	Gas Constant
gr	Rate of gas consumption ($mole/m^3$ s)
T	Temperature (K)
t	Time (s)
V	Volume (m^3)
v	Molar volume (Cm^3/mol)
W	Formation energy of nucleus (J)
Z	Longitudinal coordinate (m)
z	Zeldovich factor equation (8)

Greek Letters

ε	Kinetics parameter
μ	Chemical potential (J)
ρ	Density (kg/m^3)
σ	Surface energy (J/m^2)
ψ	Shape factor

Subscripts

e	Equilibrium
h	Hydrate
I	Counter
p	particle
w	Water
h	Hydrate phase
W	Water
R	Reactor

Superscript

s

aq.	Aqueous phase
g	Gas phase

Chapter 1- Introduction

1- Introduction

Kinetics of hydrate formation is a key parameter in the development of the mathematical models for the simulation purposes. Further, a new kind of hydrate inhibitors were developed which are based on the kinetics of hydrate formation. Hydrate inhibition is vital in the protection of gas transportation lines from blockage or damage by the hydrate

In recent years, some applications have been developed such as gas storage, water desalination, gas transportation and carbon dioxide sequestration which are based on gas hydrate formation. Hydrate promotion is an interesting item in designing hydrate production processes which can be used in the above applications.

Most of the previous studies in this matter are limited to the batch system for gas hydrate formation. But in this study, hydrate formation of carbon dioxide, propane and a mixture of methane and propane have been investigated in a recirculating flow loop experimentally and theoretically. A set of mathematical models have been developed to simulate the process of hydrate formation in the flow loop. The predicted gas consumptions are compared with the experimental data at operating temperatures and pressures of 3-8 °C and 1-5 MPa. Further, the kinetics parameters are analyzed to study their effects on the formation rates.

Complete literature reviews of gas hydrate formation are presented in chapter 1, the mathematical models are described in the chapter 2 and experimental works are presented in chapter 3. Simulation of hydrate formation is presented in chapter 4 and in chapter 5 the results of the experimental works and mathematical models are described. In the last section, conclusion is presented.

The two first sections of chapter 1 give an introduction to the microscopic structures of gas hydrates and to the thermodynamic conditions where hydrates may form. The fundamental mechanisms of hydrate formation are reviewed in Section 1.3. The driving force for hydrate formation is discussed in Section 1.4.

Experimental studies of the rate of methane, ethane and propane hydrate formation are presented in Section 1.5. Studies of hydrate crystal size are reviewed in Section 1.6. Nucleation and induction time models are reviewed in section 1.7 and models and correlations of gas hydrate formation rate are reviewed in Section 1.8. Finally, the experimental setups used in the study of hydrate formation are described in Section 1.9.

1-1- Hydrate structures

Gas hydrates are crystalline solids which are more properly called clathrate hydrates to distinguish them from stoichiometric hydrates found in inorganic chemistry. The crystalline structure is composed of polyhedra of hydrogen bonded water molecules. The polyhedra form cages that contain at most one guest molecule each. The cages are stabilized by van der Waals forces between the water molecules and the enclatherated guest molecule. In extraordinary situations, two guest molecules may enter the same cage (Sloan, 1998). Only a few kinds of cages may form depending on the size of the guest molecule. These cages arrange into different hydrate structures known as structure SI, structure SII and structure SH (Sloan, 1998) as shown in figure 1-1. Methane and natural gas form SI and SII structures, respectively. In a unit cell of SI hydrate, 2 small and 6 large cages appear. The small cage, the pentagonal dodecahedron labeled 5^{12}, has 12 pentagonal faces with equal edge lengths and equal angles.

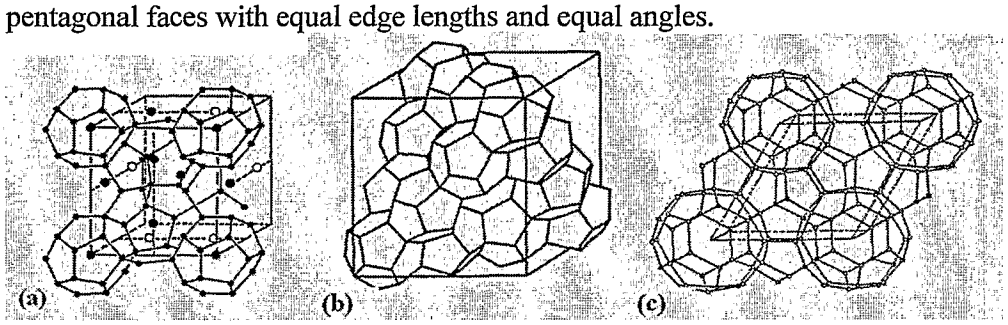

Figure 1-1- Hydrate structures known as (a) structure I (SI), (b) structure II (SII) and (c) structure H (SH) (Sloan, 1998).

The large cage, the tetrakaidecahedron, is called $5^{12}6^2$ because it has 12 pentagonal and 2 hexagonal faces. One SI unit cell has 46 water molecules and fits into a 12 Å cube. SII consists of 16 small cages and 8 large cages. Also, SII has the pentagonal dodecahedron 5^{12} as the small cage. The large cage, the hexakaidecahedron, has 12 pentagonal and 4 hexagonal faces and is therefore labeled $5^{12}6^4$. One SII unit cell has 136 water molecules and fits into a 17.3 Å cube Sloan, 1998) as shown in figure 1-2.

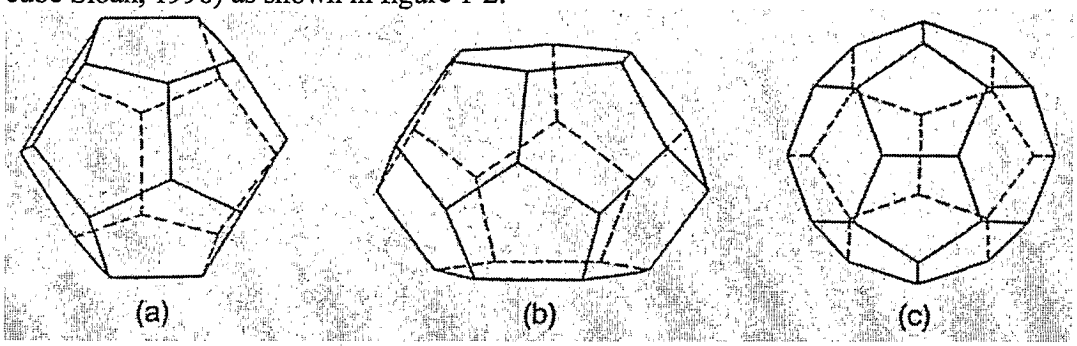

Figure 1-2- (a) Pentagonal Dodecahedron (5^{12}) (b) Tetrakaidecahedron ($5^{12}6^2$) (c) Hexakaidecahedron ($5^{12}6^4$) (Sloan, 1998)

Generally, molecules between 3.8 Å and 6.5 Å in diameter can form SI and SII hydrates if they do not contain hydrogen bonding group(s).

Depending on the size of the guest molecules, only the large cages of each structure can be occupied or both types of cages can be occupied. The small cages are never occupied alone as this is not enough to stabilize either SI or SII. However, if the small cages can be filled, the molecule will also enter the large cages as a simple hydrate species. Simple hydrates are hydrates with only one guest species (Sloan, 1998). The large cages in SI ($5^{12}6^2$) are large enough to contain molecules up to 6.0 Å in diameter, in which only ethane and carbon dioxide of the natural gas components stabilize as simple hydrates. The large cages in SII can contain molecules as large as 6.6 Å. This means that propane and iso-butane will stabilize the large cages, but leave the small cages of SII vacant. Alternatively, the small cages are filled with methane, which means that natural